KSCE Journal of Civil Engineering (2023) 27(5):2191-2201
DOI 10.1007/s12205-023-0858-6

pISSN 1226-7988, eISSN 1976-3808
www.springer.com/12205

Tunnel Engineering

The New Bubble–Slurry for Sand Conditioning during EPB Shield Tunnelling: A Laboratory Scale Study

Lu Wang[a], **Wei Zhu**[b], **Yongjin Qian**[a], **and Huitang Xing**[c]

[a]*College of Civil and Transportation Engineering, Hohai University, Nanjing 210098, China*
[b]*College of Environment, Hohai University, Nanjing 210098, China*
[c]*Jinan Rail Transit Group Co., Ltd., Jinan 250000, China*

ARTICLE HISTORY

Received 16 May 2022
Accepted 6 February 2023
Published Online 14 March 2023

KEYWORDS

EPB shield
Bubble–slurry
Stability
Sand conditioning
Permeability

ABSTRACT

Spewing is a key issue during earth pressure balance (EPB) shield tunneling in a water-rich sandy stratum. This paper proposed the bubble–slurry as a new type of soil conditioning agent. The foamability and stability of the bubble–slurry were studied, and the volume stability, fluidity, and permeability of bubble–slurry-conditioned sands with hydraulic gradient of 2 to 10 were analyzed. The stability mechanism was explored by the zeta potential and microstructure of the bubble–slurry system. The formulation of bubble–slurry with a half-life of 121 – 383 h was determined through laboratory tests. The results of soil conditioning experiments showed that the bubble–slurry-conditioned soil exhibited appropriate fluidity, excellent volume stability and low permeability in a certain period. The use of bubble–slurry can save approximately 3.0–8.2% of the slurry consumption compared with the method of slurry conditioning. The zeta potential and the distribution of slurry particles of the bubble–slurry system were key mechanisms affecting the stability of the bubble–slurry. The high absolute value of zeta potential of the system increases the dispersion of bubbles, and the slurry particles uniformly distributed on the bubble liquid film and in the Plateau boundary are conducive to enhancing the anti-disturbance ability and inhibiting the decay of bubbles.

1. Introduction

The earth pressure balance (EPB) shield is a commonly used boring machine for urban tunnel owing to its high degree of mechanization, high construction safety, low environmental impact, low cost, and simple operation compared with slurry shields. EPB shields traverse to various strata from a soft clay to sandy soil and gravel soil with high permeability. However, when the EPB shields excavate sand and gravel strata with abundant groundwater, it is essential to add foam, slurry, and polymer to ensure the chamber soil in the plastic flow state to balance the earth and water pressure on the excavation surface, and avoid several issues, such as the spewing and surface settlement (Zhu et al., 2004; Peila, 2014; Zheng et al., 2015; Avunduk et al., 2021).

The fluidity and permeability of soil are the key parameters to judge whether the soil is in the plastic flow state. The slump test is widely used to measure the fluidity of the excavated soil. Budach and Thewes (2015), Kim et al. (2019), and Lee et al. (2022) proposed a suitable slump value of 100 – 200 mm for the soil in plastic flow state based on laboratory experiments and engineering experience. The excavated soil in the pressure chamber of EPB shield maintains low permeability. Wilms (1995) suggested that the soil permeability coefficient should be less than 1×10^{-3} cm/s to prevent spewing in water-rich strata. Budach and Thewes (2015) noted that the permeability coefficient of the conditioned soil should be less than 1×10^{-3} cm/s for more than 90 min.

Foam is the most widely used soil conditioning agent with lubricating properties that can separate and reduce friction between soil particles, and foam has wide adaptability in improving soil fluidity (Quebaud et al., 1998; Ye et al., 2017; Kim et al., 2019; Wan et al., 2021). However, the performance of the foam-conditioned sand was found to be significantly affected by the groundwater pressure and soil particle size. Hu et al. (2020) found that as hydraulic gradient increases, the time required for water to penetrate throughout the foam-conditioned sand decreases.

CORRESPONDENCE Wei Zhu ✉ zhuweiteam.hhu@gmail.com College of Environment, Hohai University, Nanjing 210098, China

Huang et al. (2019) pointed out that an increase in the effective grain size of soil can greatly increase the initial permeability coefficient of conditioned soil. Therefore, it is difficult to control spewing when using only foam (Bezuijen, 2012; Mori, 2016). When EPB shield is used for tunneling in water-rich and high-permeability strata, foam is often used in conjunction with other additives to condition excavated soil, such as slurry and polymers (Xu et al., 2020; Yang et al., 2020; Li et al., 2022). However, foam and slurry are separately mixed with soil, and some bubbles may break upon contact with soil particles and free water, thereby reducing the final filling rate of the soil pores. If the bubbles and slurry can be compounded into a new type conditioning agent in which the bubbles are evenly dispersed and wrapped by the slurry, and its conditioning effect is superior to the traditional foam and slurry conditioning, especially in the case of high-water pressure and coarse-grained soil, it has a positive impact on the field of soil conditioning of EPB shield. Based on this idea, a new material with bubbles evenly dispersed in the slurry was proposed in this study, which is referred to as "bubble–slurry". The main purpose is to effectively reduce the permeability of coarse-grained soil. Bubble–slurry is a three-phase system, and its stability is critical to the conditioning effect. Studies have noted a synergy between solid particles and surfactants, and the significantly improved stability of bubbles in solid–liquid–gas phases under suitable conditions (Hill and Eastoe, 2017; Zhong et al., 2018; Wang et al., 2020). However, the ideal conditions for solid particles and surfactants to delay bubble decay remain unclear (Arriaga et al., 2012). Moreover, the types of slurry and surfactant that can be used to obtain a stable bubble–slurry system are still unknown.

Thus, the bubble–slurry is proposed as a new soil conditioning agent. The calcium bentonite slurry and two common commercial surfactants were used to prepare different bubble–slurry systems, and the foamability and stability of bubble–slurry was investigated. The conditioning effect was systematically evaluated using volume stability, slump, and permeability tests of the bubble–slurry-conditioned sand. The stability mechanism of the bubble–slurry was explored based on the zeta potential and microstructure of the bubble–slurry system. The results indicate that the bubble–slurry has excellent stability and the ability to improve sand.

2. Materials and Methods

2.1 Materials

2.1.1 Bentonite and Surfactant

The calcium bentonite used in this study has a montmorillonite content of 60.15% and an expansion index of 11 mL. Two types of commercial foaming agents were used: an animal protein surfactant (APS) with keratin as the main raw material, which is an amphoteric surfactant with density of 1.09 g/cm^3 and pH of 6.8, and a synthetic surfactant (SS) with fatty alcohol polyoxyethylene ether sodium sulfate as the main raw material, which is an anionic surfactant with density of 1.07 g/cm^3 and pH of 7.3.

2.1.2 Sand

According to the sand excavated from the ZDK21+700 to

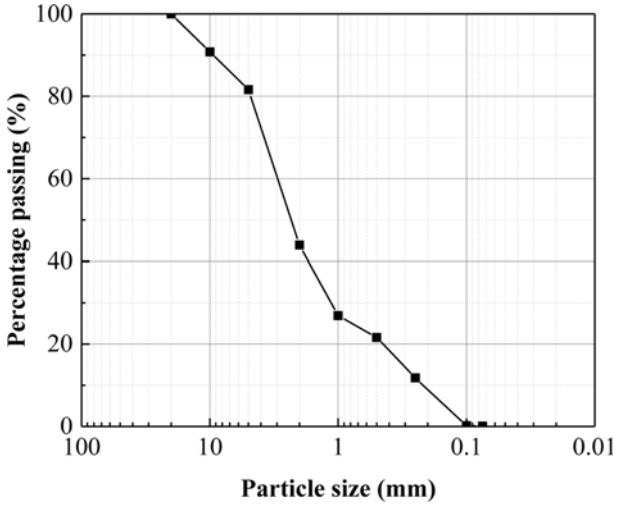

Fig. 1. Grain Size Distribution of the Sand Sample

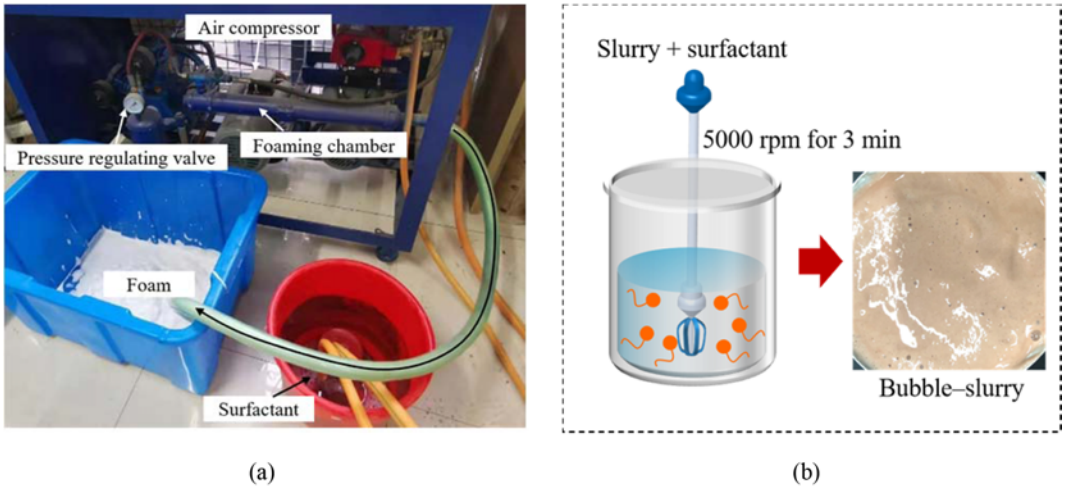

Fig. 2. Preparation of: (a) Foam, (b) Bubble–Slurry

ZDK22+600 section of the left line of the Hengli to Panyu Square section tunnel of Guangzhou metro line 18, the particle size distribution of the test sand was d_{10} = 0.22 mm, d_{50} = 2.32 mm, and d_{90} = 9.72 mm, as shown in Fig. 1. The water content of sand was 10% and the initial permeability coefficient k_0 was 4.82 × 10^{-3} cm/s.

2.2 Test Methods

2.2.1 Preparation of Foam, Slurry, and Bubble–Slurry

The foam generating device shown in Fig. 2(a) was used to prepare foam. The foaming chamber was filled with glass balls with a diameter of 0.2 – 4 mm. The surfactant solution produced foam under a pressure of 0.2 MPa.

The calcium bentonite with a mass percentage of 10 – 30% was dispersed in water at 25°C. Subsequently, anhydrous sodium carbonate powder (4% of bentonite in mass) was added to improve the expansibility of calcium bentonite in water. A hand-held mechanical agitator was used to stir the mixture at 700 rpm for 20 min, and the mixture was allowed to stand for 24 h to form a stable suspended slurry. The rheological curve of slurry was measured with a rotary viscometer (NXS-11A, Chengdu Instrument Factory, China), and the operation details were obtained from Min et al. (2018). The plastic viscosity of slurry was obtained by fitting the rheological curve with Bingham fluid model. A Malvern Mastersizer 2000 instrument (Malvern Instruments Ltd., Worcestershire, UK) was used to measure the particle size distribution of slurry and obtain the median particle size (d_{50}) of slurry. The basic properties of bentonite slurry are listed in Table 1.

When preparing the bubble–slurry, the slurry and surfactant were mixed according to different mass ratios to form a 100 mL mixture. High speed mixing method was commonly used to prepare three-phase foam (Wang et al., 2020); therefore, the mixture of surfactant and slurry was mixed at 5,000 rpm for 3 min to produce bubble–slurry (Fig. 2(b)).

2.2.2 Foamability and Stability of the Bubble–Slurry

The foam expansion ratio (FER) and bubble–slurry expansion ratio (BSER) were used to evaluate the foamability of foam and bubble–slurry, respectively. FER is the ratio of the volume of foam to the volume of liquid before foaming, which can be calculated using Eq. (1) to evaluate the foamability of traditional aqueous foam (EFNARC, 2005). Similarly, BSER is the ratio of the bubble–slurry volume to mixed liquid volume before foaming (Eq. (2)), and the bubble volume ratio (BVR) is the ratio of the bubble volume to bubble–slurry volume. Assuming that the volume of liquid before foaming was 1, Eq. (3) could be obtained using simple transformation.

Table 1. Basic Properties of the Bentonite Slurry

Slurry identifier	c_s/%	Density/ g/cm^3	Plastic viscosity/Pa·s	d_{50}/μm
SL-1	10	1.05	0.011	8.47
SL-2	15	1.14	0.015	9.91
SL-3	20	1.17	0.131	10.07
SL-4	25	1.18	0.232	10.01
SL-5	30	1.20	0.667	10.287

Note: d_{50} = median particle size (μm).

The stability of foam and bubble–slurry can be evaluated using their half-life values. After foaming, the sample was injected into a 1,000 mL graduated cylinder, and the initial volume and the change in volume with time were measured. The half-life of the foam and bubble–slurry is the time required for the bubble volume in the system to decay to half its initial value. The slurry concentration c_s, APS concentration c_{aps}, and SS concentration c_{ss} were calculated using Eqs. (4) – (6).

$$FER = \frac{V_F}{V_L}, \tag{1}$$

$$BSER = \frac{V_{BS}}{V_L}, \tag{2}$$

$$BVR = \frac{V_B}{V_{BS}} = \frac{BSER - 1}{BSER}, \tag{3}$$

$$c_s = \frac{m_b}{m_s}, \tag{4}$$

$$c_{aps} = \frac{m_{aps}}{m_L} + \frac{m_{aps}}{m_{aps} + m_s}, \tag{5}$$

$$c_{ss} = \frac{m_{ss}}{m_L} = \frac{m_{ss}}{m_{ss} + m_s}, \tag{6}$$

where V_F is the volume of the foam (cm^3), V_L is the volume of the mixed liquid before foaming (cm^3), V_{BS} is the volume of the bubble–slurry (cm^3), V_B is the volume of bubbles (cm^3), m_b is the weight of bentonite (g), m_s is the weight of slurry (g), m_{aps} is the weight of *APS* (g), m_{ss} is the weight of *SS* (g), and m_L is the weight of the mixed liquid (g).

2.2.3 Sand Conditioning Tests

The sand conditioning tests included volume stability, slump, and permeability test of conditioned sand. Various agents and sand were mixed according to different volume ratios for 3 min; subsequently, the volume stability test was performed by placing the conditioned sand in a pressurized plexiglass cylinder with inner diameter of 12 cm and height of 20 cm, and the top cover of the cylinder was connected with the air compressor to apply air pressure (P) to the conditioned sand. The change in conditioned sand volume with time under atmospheric pressure (P = 0) and P = 1 bar was recorded, and the ratio of the reduced conditioned sand volume to its initial volume after 24 h was the volume change rate of the conditioned sand in 24 h. Further, the fluidity of the conditioned sand was evaluated by the standard slump test (ASTM, 2003).

The permeability coefficient of the soil was measured using a self-made permeameter with a height and diameter of 60 and 12 cm, respectively. The permeability test process is based on ASTM

(2006). First, a specific amount of dry soil was mixed with the designed amount of water for more than 3 min to achieve a uniform mixture. A specific amount of the conditioning agent was then mixed with the soil for 3 min. Subsequently, the conditioned sand was poured into the permeameter and was filled with water. The above procedure was completed within 10 min. The top of the permeameter was sealed with a flange, which was connected with the water tank through a flexible tube. The top cover of the water tank was connected to the air compressor and the water pressure (P_w) was adjusted by applying air pressure to the water surface. The water level gradually dropped during permeability test; therefore, the air pressure was manually increased in real time according to the reduction in water level to maintain the P_w on the top of the soil constant. In this study, the P_w were set to 0.01, 0.02, 0.03, and 0.05 MPa, and the corresponding hydraulic gradients i were approximately equal to 2, 4, 6, and 10, respectively.

At the beginning of permeability test, the height of the soil under P_w was recorded, the seepage volume over a period was recorded, and the test lasted for 90 min (Budach and Thewes, 2015). According to the height of the soil, water-level difference, seepage water volume, and time, the permeability coefficient of the soil can be calculated using the following formula:

$$k = \frac{QL}{AHt}, \tag{7}$$

where k is the permeability coefficient of the soil (cm/s), Q is the infiltration water volume at time t (cm^3), L is the height of the sample under water pressure (cm), A is the cross-sectional area of the sample (cm^2), H is the water-level difference (cm), and t is the infiltration time (s).

2.2.4 Zeta Potential and Microstructure

A zeta potentiometer (Nano ZS90, Malvern Instruments Ltd., UK) and optical microscope (Scope. A1, Carl Zeiss Corporation, Oberkochen, Germany) with a digital camera (AxioCam ICc 3) were used to analyze the zeta potential and microstructure of the bubble–slurry system to determine its stabilization mechanism. In the zeta potential test, the zeta potential was measured through electrophoretic light scattering. Therefore, the zeta potential for an aqueous solution of the surfactant can be directly measured. However, for a mixture of the slurry and surfactant with poor light transmittance, its supernatant was taken for the measurement (Zhao et al., 2016). In this study, a centrifuge device (TW5A-

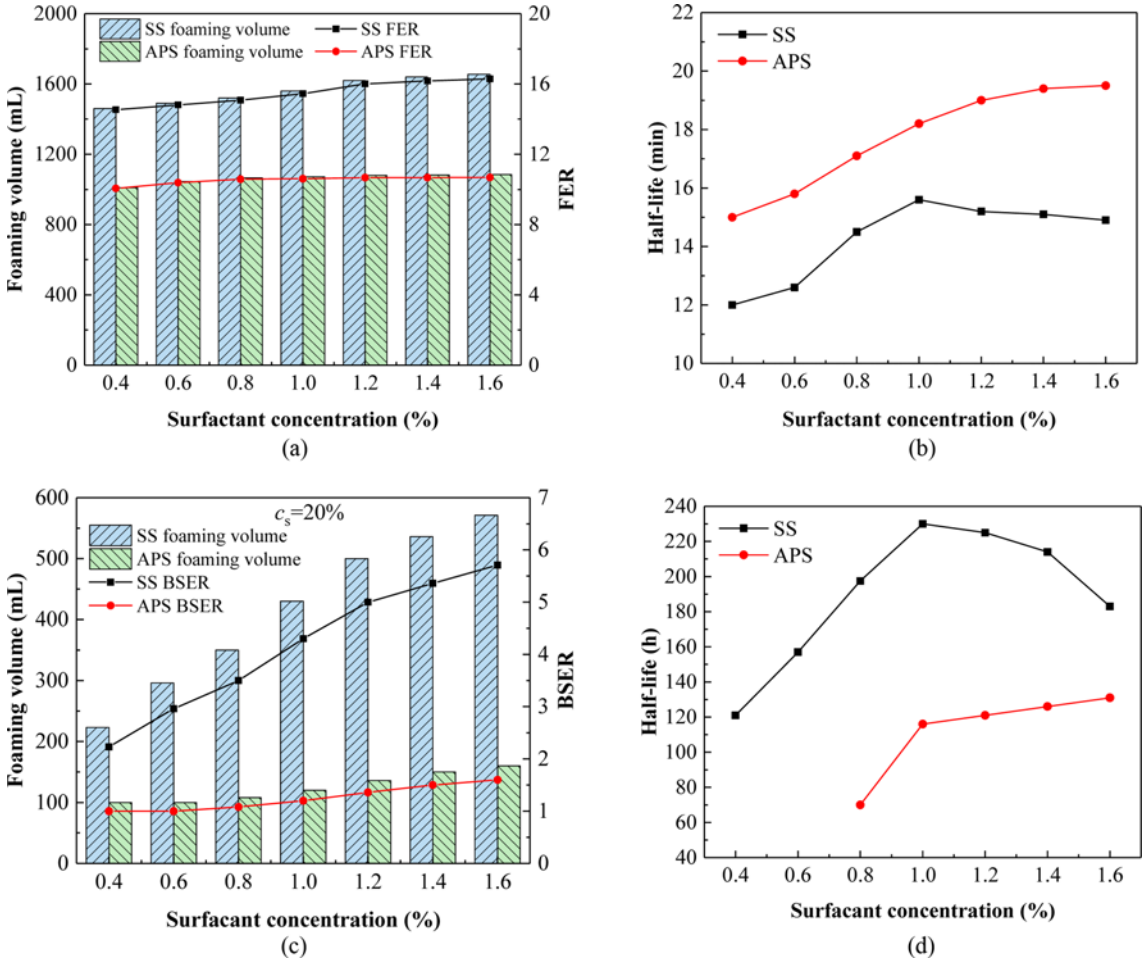

Fig. 3. The Foamability and Stability of Surfactants in Water or Slurry: (a) Foamability, (b) Foam Half-Life of SS and APS in Water at Concentrations Ranging from 0.4% to 1.6%, (c) Foamability, (d) Bubble–Slurry Half-Life of SS and APS in SL-3 Slurry at Concentrations Ranging from 0.4% to 1.6%

WS, Changzhou Jintan Jingda Instrument Manufacturing Co., Ltd, China) was used to centrifuge the mixture of the slurry and surfactant at 1,000 rpm for 1 min to obtain the supernatant; then, its zeta potential was measured. The test temperature was set to 25°C. Each sample was measured thrice with their average values reported.

In the microstructure test, the pure foam was placed on the glass slide immediately after preparation, and the foam was gently scraped with a thin glass sheet to make it as flat as possible and then was observed with an optical microscope. However, the bubble–slurry has poor light transmittance. Therefore, it was freeze-dried before observation under an optical microscope, the influence on the distribution of bentonite particles was negligible. First, lay 10 mL sample in a metal container, then put it in a freeze dryer (LGJ–18, Beijing Songyuan Huaxing Technology Develop Co., Ltd., China) and wait for the temperature to drop below -50°C with strictly seal. Then, turn on the vacuum pump till the vacuum is below 20 Pa for approximately 24 h to obtain a bubble–slurry freeze-dried sample. Finally, place the freeze-dried sample on the glass slide and observe it under an optical microscope.

3. Results

3.1 Foamability and Stability of the Bubble–Slurry System

3.1.1 Effect of the Surfactant Type and Concentration on the Foamability and Stability

The foamabilities and stability of APS and SS in the slurry were compared with those in water, as shown in Fig. 3. The two surfactants exhibited good foaming performance in water, in which the foaming volume increases with the increase of the surfactant concentration (Fig. 3(a)). Meanwhile, the foam half-life with SS can reach approximately 15 min, whereas that with APS can reach approximately 20 min (Fig. 3(b)). When c_{ss} was 1.2 – 1.6%, the half-life of foam slightly decreased. It was mainly because the FER exceeded 16, the foam was dry and the liquid film was thin, and bubbles were more likely to burst, resulting in a certain degree of half-life reduction.

However, APS exhibited poor foaming ability in SL-3 slurry, the BSER did not reach 2.0 when the c_{aps} increased to 1.6% (Fig. 3(c)). Meanwhile, although the foaming effect of SS in the SL-3 slurry is lower than that in water, an BSER of approximately 6 could be achieved with an increase in the c_{ss}. As shown in Fig. 3(d), the half-life of the bubble–slurry with the c_s of 20% generated by the two surfactants could reach 100 – 200 h, which is significantly more stable than foam. Moreover, the bubble–slurry prepared using SS exhibited better stability than that prepared using APS. Therefore, SS exhibited better foamability and stability in the SL-3.

3.1.2 Effect of the Slurry Concentration on Foamability and Stability

As shown in Fig. 4, the foamability of mixture of slurry and surfactant decreased with increasing c_s. Meanwhile, the foamability of APS and SS significantly decreased when c_s were greater than 15% and 25%, respectively. When c_s was 30%, the BSER of bubble–slurry made of SS was 1.3 and the BVR was 23.08% (Fig. 4(a)). A higher c_s prolongs the half-life of the bubble–slurry (Fig. 4(b)). Moreover, the stability of the SS bubbles is better than that of the APS bubbles. Particularly, APS did not foam in the slurry when c_s exceeds 20%, thus, data on the half-life of the APS bubbles at high-concentration slurries are not available.

3.2 Formulation of the Bubble–Slurry

Based on the foamability and half-life of the bubble–slurry with two types surfactants, SS exhibits the superior foamability with more stable bubbles; therefore, it was selected as the foaming agent in the bubble–slurry preparation for the subsequent experiments. Moreover, the stability of the bubble–slurry increased with the increase in the c_s; however, the bubble–slurry systems with c_s over 30% exhibit poor foamability. Hence, the c_s of 20 – 30% was considered. Five bubble–slurry formulations were

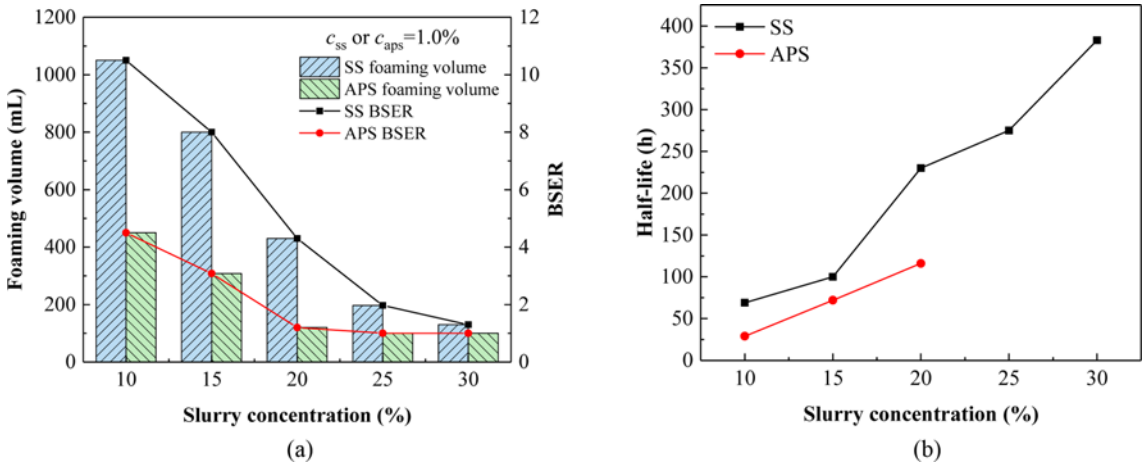

Fig. 4. Influence of the Slurry Concentration on the: (a) Foamability, (b) Bubble-Slurry Half-Life (surfactant concentration of 1.0%)

Table 2. Experimental Bubble–Slurry Formulations

ID	*BVR* / %	Half-life/ h	BSER	c_s / %	c_{ss} / %
BS-1	23.08	383	1.3	30	1.0
BS-2	49.24	275	1.97	25	1.0
BS-3	55.16	121	2.23	20	0.4
BS-4	76.74	230	4.3	20	1.0
BS-5	81.34	214	5.36	20	1.4

initially selected (Table 2) to conduct the volume stability, slump, and permeability tests of the conditioned sand.

3.3 Effect of the Bubble–Slurry on Sand Conditioning

3.3.1 Volume Stability of the Bubble–Slurry-Conditioned Sand

To verify the stability of the bubble–slurry mixed with sand, the volume stability test of the bubble–slurry-conditioned sand was carried out and compared to foam-conditioned sand at atmospheric pressure ($P = 0$) and $P = 1$ bar, as shown in Fig. 5.

With the volume addition of the agents to soil in the range of 10 – 25%, the volume change rate within 24 h of the bubble–slurry-conditioned sand (<10%) is significantly smaller than that of the foam-conditioned sand (15 – 30%) at atmospheric pressure. Considering the influence of the chamber pressure of EPB shield on the bubble–slurry, the volume stability of the bubble–slurry-conditioned sand and foam-conditioned sand under the condition of $P = 1$ bar was analyzed, as shown in Fig. 5(b). The conditioned sand stability increases at $P = 1$ bar (Wu et al., 2020), the reason is that the pressure makes the connection between the particles tighter, delaying the coarsening and collapse of the bubbles in the conditioned sand. Comparing the volume change of the five bubble–slurry formulations, a larger BVR results in a higher volume change rate of the conditioned sand. In addition, the increase in the added amount of bubble–slurry increases the soil volume change rate. Based on engineering applications, the conditioned sand is required to maintain stability within 90 min (Budach and Thewes, 2015). When $P = 1$ bar, the volume change rate within 24 h of the bubble–slurry-conditioned sand is less than 6%, which can ensure that the chamber is fully filled with conditioned soil during tunnelling, which is also conducive to reducing the infiltration of groundwater.

3.3.2 Fluidity of the Bubble–Slurry-Conditioned Sand

The fluidity of the bubble–slurry-conditioned sand was studied using the slump test, as shown in Fig. 6. The unconditioned sand has a slump of 0. With the volume addition of conditioning agents in the range of 10 – 25%, the slump value significantly increased, and the fluidity of conditioned sand increases with the increase of BVR. The fluidity of the foam-conditioned sand is greater than that of the bubble–slurry-conditioned sands. For engineering applications, the suitable slump value was between

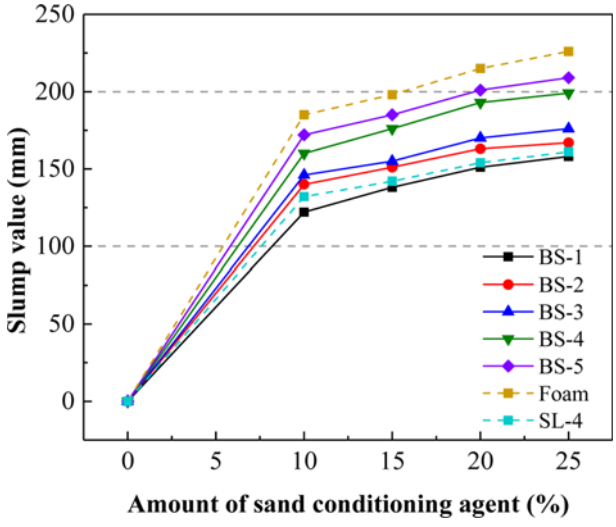

Fig. 6. Fluidity of Sands Conditioned with Different Agents

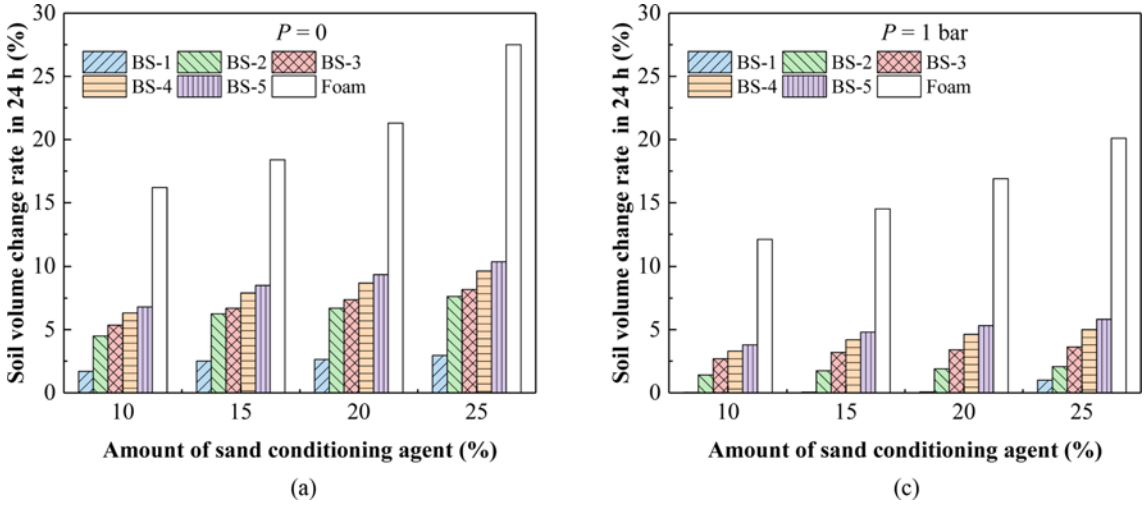

Fig. 5. Volume Stability of the Bubble–Slurry-Conditioned and Foam-conditioned Sands at: (a) $P = 0$, (b) $P = 1$ Bar

100 – 200 mm. Therefore, in terms of the addition amount, the bubble–slurry conforms to the required fluidity for engineering construction in a larger addition range.

3.3.3 Permeability of the Bubble–Slurry-Conditioned Sand

The permeability test was carried out under the water pressure P_w of 0.01 MPa (the hydraulic gradient i was 2), as shown in Fig. 7(a). In engineering applications, spewing can be prevented when the chamber soil permeability coefficient is less than 1.0×10^{-3} cm/s (Wilms, 1995; Hu et al., 2020). The permeability coefficient of the foam-conditioned sand is still greater than 1.0×10^{-3} cm/s when the foam addition amount is 25%. Compared with the use of foam as the conditioning agent, the permeability coefficient of the bubble–slurry-conditioned sand exhibited a sharp decreased. Among the several groups of bubble–slurry used in this test, BS-1 exhibited the best anti-seepage performance because of the smallest BVR and the highest c_s. When the addition amount of BS-1 is 5%, the permeability coefficient of the conditioned sand is less than 1.0×10^{-3} cm/s. The c_s of BS-2 and SL-4 is the same, the BVR of BS-2 is 49.24%, but its conditioning effect of the permeability of sand is close to that of SL-4, which means that it can save approximately 50% of slurry consumption.

To compare the difference between bubble–slurry conditioning and conventional slurry conditioning, foam conditioning, and the simultaneous use of slurry and foam (hereinafter referred to as slurry + foam conditioning), the change in the permeability coefficient with hydraulic gradient was analyzed, as shown in Fig. 7(b). According to the BVR of bubble–slurry, the amount of foam added when using slurry + foam conditioning was determined. With the increase of hydraulic gradient, the permeability coefficient of foam-conditioned sand gradually approached that of unconditioned sand, indicating that the increase of

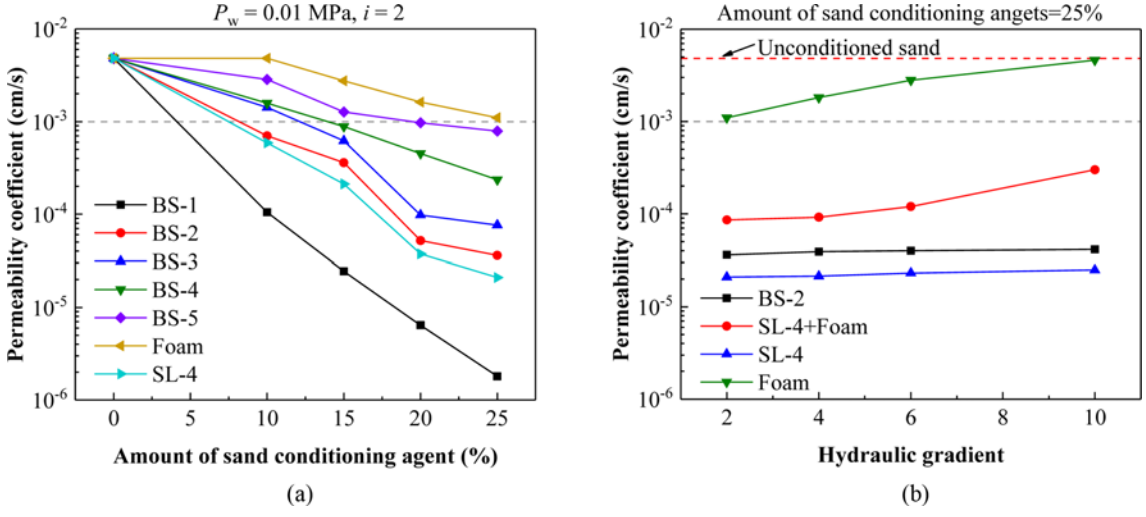

Fig. 7. The Amount of Sand Conditioning Agent and Hydraulic Gradient versus Permeability Coefficient (i = 10): (a) Amount of Sand Conditioning Agent, (b) Hydraulic Gradient

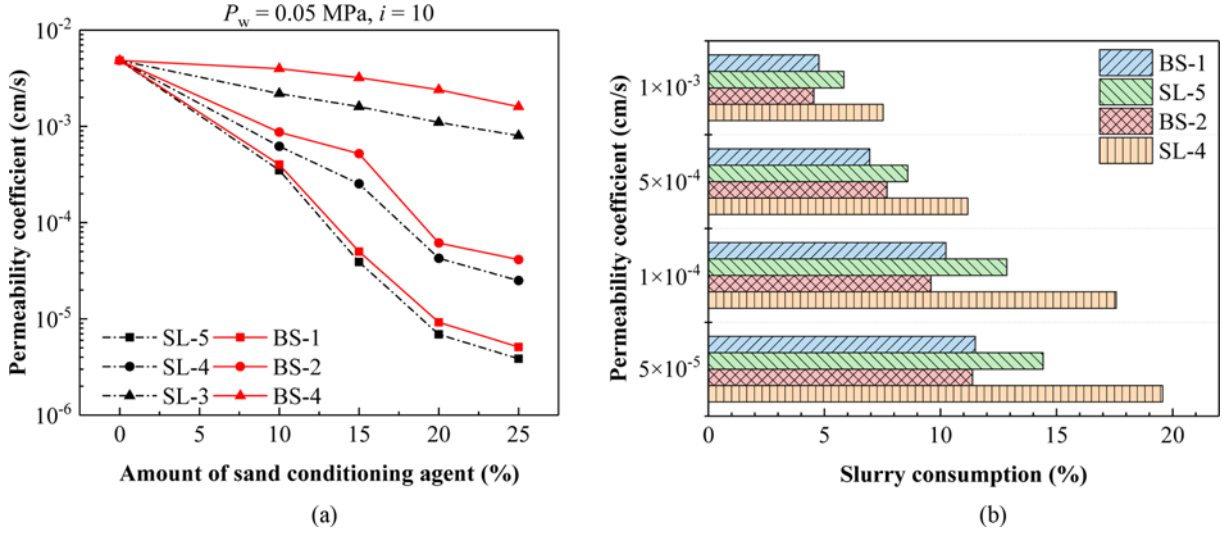

Fig. 8. The Amount of Sand Conditioning Agent and Slurry Consumption versus Permeability Coefficient (i = 10): (a) Bubble–Slurry-Conditioned and Slurry-Conditioned Sand, (b) Slurry Consumption

hydraulic gradient drives foam loss from soil pores. In the range of hydraulic gradient from 2 to 10, the permeability coefficients of the slurry-conditioned sand and the bubble–slurry conditioned sand did not change much, indicating that the bubble–slurry could exist in the sand pores stably like slurry. The permeability coefficient of the slurry + foam conditioned sand increases with the hydraulic gradient, especially after the hydraulic gradient reaches 4. The results exhibited that the impermeability of the bubble–slurry-conditioned sand was better than that of the slurry + foam conditioned sand.

3.3.4 Comparison of Slurry Consumption under High Hydraulic Gradient

The higher the hydraulic gradient is, the more prone the sand is to spewing. In order to evaluate the permeability of the bubble–slurry-conditioned sand under high hydraulic gradient, the difference in the permeability coefficient of the bubble–slurry-conditioned and slurry-conditioned sands with the equal c_s values was compared and analyzed when the hydraulic gradient reached 10, as shown in Fig. 8(a). The c_s of the bubble–slurry BS-1 (c_s = 30%), BS-2 (c_s = 25%), and BS-4 (c_s = 20%) were the same as those of the slurry SL-5, SL-4, and SL-3, respectively. At equal c_s values, the permeability coefficient of the bubble–slurry-conditioned sand is slightly larger than that of the slurry-conditioned sand. However, with the increase in the c_s, the difference in the permeability coefficients gradually decreased.

The BVR of the bubble–slurry can be used to determine the quantitative relationship between the slurry consumption and permeability coefficient of the conditioned sand. Fig. 8(b) shows the slurry consumption with respect to the permeability coefficient of the sands conditioned with different agents. The use of bubble–slurry can reduce the amount of slurry when the c_s is the same, when the permeability coefficient of the conditioned sand is reduced to 5.0×10^{-5} cm/s, the use of bubble–slurry can save about 3.0 – 8.2% of the slurry compared with the method of slurry conditioning.

4. Discussion

4.1 Stability Mechanism of the Bubble–Slurry

4.1.1 Zeta Potential of the Bubble–Slurry System and Selection of the Surfactant

The foamability and stability of the APS–bentonite slurry system is significantly lower than those of the SS–bentonite slurry system. Zeta potential plays an important role in the stability of aqueous foam and three-phase foam systems (Garbin et al., 2012; Hamedi-Shokrlu and Babadagli, 2014; Zhao et al., 2016). Fig. 9(a) shows the negative zeta potentials of SS and APS with SS exhibiting a more negative charge at the same concentrations. When c_{ss} increased, the absolute value of the zeta potential of the system increased, as shown in Fig. 9(b), indicating the increased electrostatic repulsion and dispersal between the slurry particles, which is conducive for the stability of the bubble–slurry system. However, the increase in c_{aps} significantly reduced the absolute value of the zeta potential. This is because APS is an amphoteric surfactant with both anionic and cationic hydrophilic groups. The combination of cationic hydrophilic group and the negative charge on the surface of slurry particles reduced the negative charge on the surface of particles, which increased the tendency for particle aggregation and reduced foamability and bubble–slurry stability. Notably, pH influences whether the hydrophilic group of the amphoteric surfactant is mainly anionic or cationic, and the zeta potential of APS varies with pH (Qiao et al., 2020). This aspect is beyond the scope of the current work and is worth further exploring in future studies. Therefore, for different kinds of slurries, surfactants with the zeta potentials with the same symbol and large absolute values can be selected. For the bentonite slurry, the anionic surfactant can improve the foamability and stability of the system.

4.1.2 Microstructure of the Bubble–Slurry

To reveal the mechanism behind the stability of the bubble–

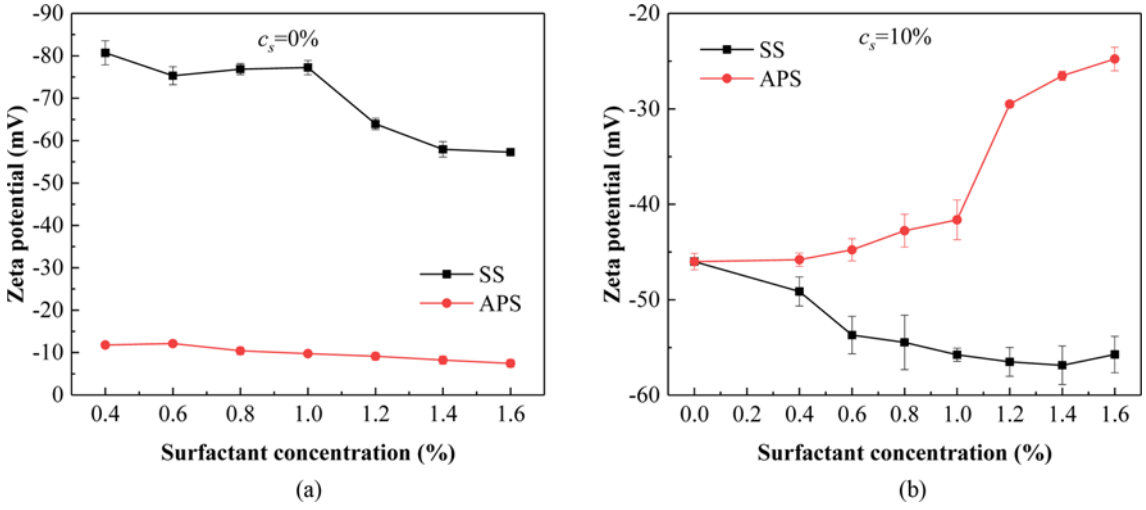

Fig. 9. Zeta Potential of the Mixed Solution with respect to the Surfactant Concentration: (a) No Slurry, (b) c_s = 10%

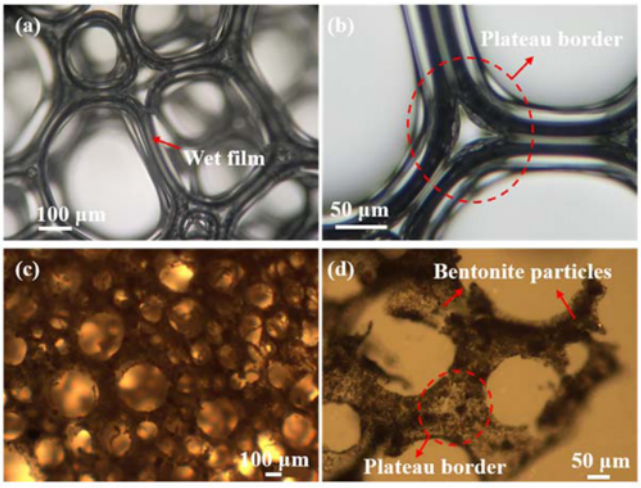

Fig. 10. Microstructure of Traditional Aqueous Foam and Bubble–Slurry Prepared Using SS: (a) Aqueous Foam and Its, (b) Plateau Boundary, (c) Bubble–Slurry after Freeze Drying (c_s = 20%, c_{ss} = 0.4%) and Its, (d) Plateau Boundary

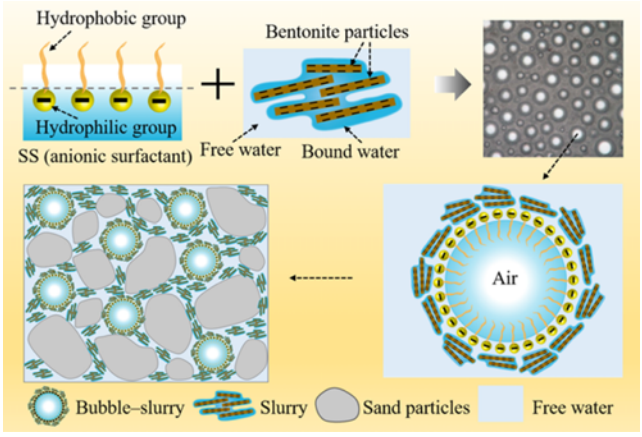

Fig. 11. Schematic Diagram of Bubble–Slurry and Its Conditioned Sand

slurry, the micromorphology of traditional aqueous foam and bubble–slurry prepared by SS were compared, as shown in Fig. 10. The bubbles of traditional aqueous foam are mostly polygonal and in contact with each other. Adjacent bubbles easily merge into larger bubbles and the liquid film is drained through the Plateau boundary under the action of gravity. However, the bentonite particles are evenly distributed at the Plateau boundary and gas–liquid interface, and the liquid film drainage is mainly controlled by viscosity rather than inertia under gravity, thus prolonging the time for liquid film drainage, and the spacing between the bubbles significantly increased, as shown in Fig. 10(c) and Fig. 10(d). Another factor affecting the drainage of liquid film is the capillary pressure that makes the adjacent bubbles merge. The capillary pressure between bubbles with particles is much smaller than that of pure foam, indicating that bentonite reduces the capillary pressure between bubbles. The disjoining pressure is the main factor affecting the stability of foam (Langevin, 2015). The absolute value of zeta potential increases after SS and bentonite particles are combined, and the electrostatic repulsion increases the disjoining pressure between bubbles. According to Sagert and Quinn (1978), the electrostatic repulsion can balance the capillary pressure and further inhibit bubble merging. This indicates the adsorption of the bentonite particles at the bubble film formed a firm viscoelastic shell around the bubbles to prevent their drainage, coarsening, and coalescence. Previous studies showed that the spatial barrier formed by the particles between the bubbles is an important factor in improving the stability of the bubbles (Carn et al., 2009; Tzoumaki et al., 2015; Zhao et al., 2016; Sheng et al., 2020; Wang et al., 2020).

4.2 Advantages the Bubble–Slurry

In practical engineering, the foam and slurry were separately mixed with the soil. However, the bubble–slurry proposed in this study is a stable system of bubbles and the bentonite slurry. Schematic diagram of bubble–slurry and its conditioned sand as shown in Fig. 11. During conditioning, the bubble–slurry was mixed with the chamber soil in the form of a whole material, and the bubbles were fully wrapped by the slurry. Therefore, once the pores of the sand are completely filled with the bubble–slurry, the seepage path of water is blocked between the pores of sand and slurry, and the pores of slurry and slurry, resulting in a low permeability. Owing to the less direct contact between the bubbles and permeating water, it is conducive to maintain the stability. Therefore, the effect of bubble–slurry conditioning is better than that of traditional slurry and foam (Fig. 7(b)), and can save the slurry consumption (Fig. 8(b)), thereby reducing the cost while having minimal impact on the subsequent treatments of the residue soil. A simple cost analysis of foam and bubble–slurry was performed. The calcium bentonite used in this study was approximately 0.15 yuan/kg, SS was approximately 5 yuan/kg, and industrial anhydrous sodium carbonate powder was approximately 3.5 yuan/kg. In actual engineering, the concentration of foaming solution is usually 3%, the FIR is 20 – 60% (Peila et al., 2019; Li et al., 2022), and FER is 10 – 15. Based on the bubble–slurry formulations in Table 2, the BSIR was 10 – 25%, and the cost of foam or bubble–slurry required for each 1 m^3 of excavated soil is listed in Table 3. Meanwhile, the surfactant is added as an admixture to the slurry to participate in foaming and simplify the injection process. During the excavation of coarse-grained soil, polymers are often used to improve the soil workability. The action mechanism of a polymer is to absorb free water and

Table 3. Cost of Foam and Bubble–Slurry

Agent	Foam	BS-1	BS-2	BS-3	BS-4	BS-5
Cost (yuan/m^3)	2.25 – 9	13.07 – 31.04	7.18 – 18.68	3.63 – 10.03	2.51 – 7.54	2.96 – 7.43

cohere fine particles. The action mechanism of bubble–slurry ensures that fine particles and bubbles cooperate to plug soil pores. Compared with the conditioning method of polymer combined with foam, the bubbles in the bubble–slurry are better protected. When there are little fine particles in coarse-grained soil, it is difficult for the cohesiveness of polymer to fully develop. The effect of polymer on the properties of bubble–slurry and its conditioned soil can be considered in future studies.

Bubble–slurry is a new type conditioning material proposed for the first time. The properties, conditioning effect, and stability mechanism of the bubble–slurry was investigated in this study; the applicability of bubble–slurry in different coarse-grained soils and engineering application will be clarified in the follow-up research.

5. Conclusions

1. SS exhibits the superior foamability with more stable bubbles in the bentonite slurry than APS. In this study, the optimized parameters range of bubble–slurry is taken as c_s of 20 – 30%, c_{ss} of 0.4 – 1.4%, BVR of 23.08 – 81.34%, BSER of 1.3 – 5.36, and half-life of 121 – 383 h.
2. Bubble–slurry can effectively improve the fluidity of sand. Furthermore, the bubble–slurry-conditioned sand exhibits excellent volume stability and low permeability in a certain period, and the effect of bubble–slurry conditioning is better than that of traditional slurry and foam. The use of bubble–slurry can reduce approximately 3.0 – 8.2% of the slurry consumption compared with slurry conditioning.
3. The mechanism of excellent stability of bubble–slurry is that the higher absolute value of zeta potential in the system increases the dispersion of bubbles. Further, the slurry particles are evenly distributed on the bubble liquid film and in the Plateau boundary, which is conducive to enhancing the anti-disturbance ability and inhibiting the decay of bubbles.

Acknowledgments

The authors would like to acknowledge the National Basic Research Program of China ('973' Program, 2015CB057803), the Fundamental Research Funds for the Central Universities (B200203081), and the Postgraduate Research and Practice Innovation Program of Jiangsu Province (KYCX20_0436).

ORCID

Lu Wang http://orcid.org/0000-0002-1826-1554
Wei Zhu http://orcid.org/0000-0002-2907-6020
Yongjin Qian http://orcid.org/0000-0001-6337-362X

References

Arriaga LR, Drenckhan W, Salonen A, Rodrigues JA, Íñiguez-Palomares R, Rio E, Langevin D (2012) On the long-term stability of foams stabilised by mixtures of nano-particles and oppositely charged short chain surfactants. *Soft Matter* 8(43):1185-1197, DOI: 10.1039/c2sm26461g

ASTM (2003) Standard test method for slump of hydraulic-cement concrete C143/C 143M-00. ASTM International, West Conshohocken, PA, DOI: 10.1520/C0143_C0143M-20

ASTM (2006) Standard test method for permeability of granular soils (constant head) D2434-68. ASTM International, West Conshohocken, PA, DOI: 10.1520/D2434-68R06

Avunduk E, Copur H, Tolouei S, Tumac D, Balci C, Bilgin N, Shaterpour Mamaghani A (2021) Possibility of using torvane shear testing device for soil conditioning optimization. *Tunnelling and Underground Space Technology* 107:103665, DOI: 10.1016/j.tust.2020.103665

Bezuijen A (2012) Foam used during EPB tunnelling in saturated sand, parameters determining foam consumption. Proceedings WTC 2012, Bangkok, Thailand, 267-269

Budach C, Thewes M (2015) Application ranges of EPB shields in coarse ground based on laboratory research. *Tunnelling and Underground Space Technology* 50:296-304, DOI: 10.1016/j.tust.2015.08.006

Carn F, Colin A, Pitois O, Vignes-Adler M, Backov R (2009) Foam drainage in the presence of nanoparticle-surfactant mixtures. *Langmuir* 25(14):7847-7856, DOI: 10.1021/la900414q

EFNARC (European Federation for Specialist Construction Chemicals and Concrete Systems) (2005) Specifications and guidelines for the use of specialist products for mechanized tunnelling (TBM) in soft ground and hard rock. In Recommendation of European federation of producers and contractors of specialist products for structures. Farnham, UK: EFNARC, http://www.efnarc.org/publications.html

Garbin V, Crocker JC, Stebe KJ (2012) Nanoparticles at fluid interfaces: Exploiting capping ligands to control adsorption, stability and dynamics. *Journal of Colloid and Interface Science* 387(1):1-11, DOI: 10.1016/j.jcis.2012.07.047

Hamedi-Shokrlu Y, Babadagli T (2014) Stabilization of nanometal catalysts and their interaction with oleic phase in porous media during enhanced oil recovery. *Industrial & Engineering Chemistry Research* 53(20):8464-8475, DOI: 10.1021/ie4042033

Hill C, Eastoe J (2017) Foams: From nature to industry. *Advances in Colloid and Interface Science* 247:496-513, DOI: 10.1016/j.cis.2017.05.013

Hu QX, Wang SY, Qu TM, Xu T, Huang S, Wang HB (2020) Effect of hydraulic gradient on the permeability characteristics of foam-conditioned sand for mechanized tunnelling. *Tunnelling and Underground Space Technology* 99, DOI: 10.1016/j.tust.2020.103377

Huang ZQ, Wang C, Dong JY, Zhou JJ, Yang JH, Li YW (2019) Conditioning experiment on sand and cobble soil for shield tunneling. *Tunnelling and Underground Space Technology* 87:187-194, DOI: 10.1016/j.tust.2019.02.011

Kim T, Kim B, Lee K, Lee I (2019) Soil conditioning of weathered granite soil used for EPB shield TBM: A laboratory scale study. *KSCE Journal of Civil Engineering* 23(4):1829-1838, DOI: 10.1007/s12205-019-1484-1

Langevin D (2015) Bubble coalescence in pure liquids and in surfactant solutions. *Current Opinion in Colloid & Interface Science* 20(2):92-97, DOI: 10.1016/j.cocis.2015.03.005

Lee H, Kwak J, Choi J, Hwang B, Choi H (2022) A lab-scale experimental approach to evaluate rheological properties of foam-conditioned soil for EPB shield tunnelling. *Tunnelling and Underground Space Technology* 128:104667, DOI: 10.1016/j.tust.2022.104667

Li S, Wan Z, Zhao S, Ma P, Wang M, Xiong B (2022) Soil conditioning tests on sandy soil for earth pressure balance shield tunneling and

field applications. *Tunnelling and Underground Space Technology* 120:104271, DOI: 10.1016/j.tust.2021.104271

Min FL, Song HB, Zhang N (2018) Experimental study on fluid properties of slurry and its influence on slurry infiltration in sand stratum. *Applied Clay Science* 161:64-69, DOI: 10.1016/j.clay.2018.03.028

Mori L (2016) Advancing understanding of the relationship between soil conditioning and earth pressure balance tunnel boring machine chamber and shield annulus behavior. PhD Thesis, Colorado School of Mines, Ann Arbor, USA, http://hdl.handle.net/11124/170474

Peila D (2014) Soil conditioning for EPB shield tunnelling. *KSCE Journal of Civil Engineering* 18(3):831-836, DOI: 10.1007/s12205-014-0023-3

Peila D, Martinelli D, Todaro C, Luciani A (2019) Soil conditioning in EPB shield tunnelling – an overview of laboratory tests. *Geomechanics and Tunnelling* 12(5):491-498, DOI: 10.1002/geot.201900021

Qiao X, Miller R, Schneck E, Sun K (2020) Influence of pH on the surface and foaming properties of aqueous silk fibroin solutions. *Soft Matter* 16(15):3374-3695, DOI: 10.1039/c9sm02372k

Quebaud S, Sibai M, Henry JP (1998) Use of chemical foam for improvements in drilling by earth-pressure balanced shields in granular soils. *Tunnelling and Underground Space Technology* 13(2):173-180, DOI: 10.1016/S0886-7798(98)00045-5

Sagert NH, Quinn MJ (1978) Coalescence of gas-bubbles in dilute aqueous-solutions. *Chemical Engineering Science* 33(8):1087-1095, DOI: 10.1016/0009-2509(78)85014-3

Sheng Y, Xue M, Zhang S, Wang Y, Zhai X, Zhao Y, Ma L, Liu X (2020) Role of nanoparticles in the performance of foam stabilized by a mixture of hydrocarbon and fluorocarbon surfactants. *Chemical Engineering Science* 228:115977, DOI: 10.1016/j.ces.2020.115977

Tzoumaki MV, Karefyllakis D, Moschakis T, Biliaderis CG, Scholten E (2015) Aqueous foams stabilized by chitin nanocrystals. *Soft Matter* 11(31):6245-6253, DOI: 10.1039/c5sm00720h

Wan Z, Li S, Yuan C, Zhao S, Wang M, Lu Q, Hou W (2021) Soil conditioning for EPB shield tunneling in silty clay and weathered mudstone. *International Journal of Geomechanics* 21(9), DOI: 10.1061/(ASCE)GM.1943-5622.0002119

Wang T, Fan H, Yang W, Meng Z (2020) Stabilization mechanism of fly ash three-phase foam and its sealing capacity on fractured reservoirs. *Fuel* 264:116832, DOI: 10.1016/j.fuel.2019.116832

Wilms J (1995) Zum einfluss der eigenschaften des stützmediums auf das verschleißverhalten eines erddruckschildes. PhD Thesis, Gesamthochschule Essen University, Nordrhein-Westfalen, Germany

Wu Y, Nazem A, Meng F, Mooney MA (2020) Experimental study on the stability of foam-conditioned sand under pressure in the EPBM chamber. *Tunnelling and Underground Space Technology* 106:103590, DOI: 10.1016/j.tust.2020.103590

Xu Q, Zhang L, Zhu H, Gong Z, Liu J, Zhu Y (2020) Laboratory tests on conditioning the sandy cobble soil for EPB shield tunnelling and its field application. *Tunnelling and Underground Space Technology* 105:103512, DOI: 10.1016/j.tust.2020.103512

Yang Y, Li X, Su W (2020) Experimental investigation on rheological behaviors of bentonite- and cmc-conditioned sands. *KSCE Journal of Civil Engineering* 24(6):1914-1923, DOI: 10.1007/s12205-020-2035-5

Ye X, Wang S, Yang J, Sheng D, Xiao C (2017) Soil conditioning for EPB shield tunneling in argillaceous siltstone with high content of clay minerals: Case study. *International Journal of Geomechanics* 17(4):5016002, DOI: 10.1061/(ASCE)GM.1943-5622.0000791

Zhao G, Dai CL, Wen DL, Fang JC (2016) Stability mechanism of a novel three-phase foam by adding dispersed particle gel. *Colloids and Surfaces a-Physicochemical and Engineering Aspects* 497:214-224, DOI: 10.1016/j.colsurfa.2016.02.037

Zheng G, Dai X, Diao Y (2015) Parameter analysis of water flow during EPBs tunnelling and an evaluation method of spewing failure based on a simplified model. *Engineering Failure Analysis* 58:96-112, DOI: 10.1016/j.engfailanal.2015.08.033

Zhong X, Liu D, Shi X, Zhao H, Pei C, Zhu T, Shao M, Zhang F (2018) Characteristics and functional mechanisms of clay-cement stabilized three-phase nitrogen foam for heavy oil reservoir. *Journal of Petroleum Science and Engineering* 170:497-506, DOI: 10.1016/j.petrol.2018.05.063

Zhu W, Qin J, Wei K (2004) Research on the mechanism of the spewing in the EPB shield tunnelling. *Chinese Journal of Geotechnical Engineering* 26(5):589-593, DOI: 10.3321/j.issn:1000-4548.2004.05.003